



## Bromate removal from water samples using strongly basic anion exchange resin Amberlite IRA-400: kinetics, isotherms and thermodynamic studies

Mu. Naushad<sup>a,\*</sup>, Mohammad Rizwan Khan<sup>a,\*</sup>, Zeid Abdullah ALOthman<sup>a</sup>,  
Md. Rabiul Awual<sup>b</sup>

<sup>a</sup>Department of Chemistry, College of Science, King Saud University, Bld#5, Riyadh, Saudi Arabia, Tel. +966 14674198; emails: [mnaushad@ksu.edu.sa](mailto:mnaushad@ksu.edu.sa) (M. Naushad), [mrkhan078@ksu.edu.sa](mailto:mrkhan078@ksu.edu.sa) (M.R. Khan), [zaothman@ksu.edu.sa](mailto:zaothman@ksu.edu.sa) (Z.A. ALOthman)

<sup>b</sup>Actinide Coordination Chemistry Group, Quantum Beam Science Center, Japan Atomic Energy Agency (SPring-8), Hyogo 679 5148, Japan, Tel. +81 791582642; email: [awual.rabiul@jaea.go.jp](mailto:awual.rabiul@jaea.go.jp)

Received 6 November 2014; Accepted 1 January 2015

### ABSTRACT

The removal of bromate ( $\text{BrO}_3^-$ ) from aqueous medium by Amberlite IRA-400 anion exchange resin was explored in order to identify the capability of this resin to remove bromate from real water samples. The effects of several physicochemical parameters such as contact time, initial  $\text{BrO}_3^-$  concentration, initial pH, and temperature were studied. The concentration of  $\text{BrO}_3^-$  was determined using ultra-performance liquid chromatography–tandem mass spectrometry. The adsorption kinetics and isotherms were well fitted by pseudo-second-order model and Freundlich model, respectively. The adsorption was evaluated thermodynamically and the results showed the endothermic nature of  $\text{BrO}_3^-$  adsorption as the value of  $\Delta H^\circ$  was positive. The negative values of  $\Delta G^\circ$  revealed the spontaneity of process. The analytical application of Amberlite IRA-400 for real water sample analysis was studied with very promising results.

*Keywords:* Water samples; ( $\text{BrO}_3^-$ ); Adsorption; Kinetics; Thermodynamics

### 1. Introduction

Bromate ( $\text{BrO}_3^-$ ) has been identified in drinking water as a byproduct, originated from the reaction of the ozonation disinfection process [1]. The ozonation disinfection process tends to oxidize bromide (natural constituents of the source water) to  $\text{BrO}_3^-$  or when chlorinated water is exposed to sunlight [2]. Nevertheless, the ozonation disinfection process has the advantage of being able to control *Cryptosporidium parvum* zoonotic parasitic protozoan, and its oocysts are refractory to the majority of disinfectant chemicals [3].

Along with  $\text{BrO}_3^-$ , the environmental protection agency (EPA) has recognized, haloacetic acids, chlorite, and trihalomethanes as substantial disinfection byproducts in drinking water [1].  $\text{BrO}_3^-$  is known to be a strong oxidant and is chemically reactive which caused cancer, diarrhea, abdominal pain, nausea, anuria, vomiting, pulmonary edema, hemolytic anemia, and central nervous system depression [4–7]. Based on carcinogenicity, the maximum contaminant level goal for  $\text{BrO}_3^-$  has set at zero  $\mu\text{g L}^{-1}$  level by EPA in drinking water. Nevertheless, the maximum contaminant level has set at  $10 \mu\text{g L}^{-1}$  in drinking water, based on the practical quantification limit [8]. The listing was based on the

\*Corresponding authors.

EPA and the World Health Organization has classified  $\text{BrO}_3^-$  as a Group B2 substance (probable human carcinogen) with adequate information of carcinogenicity in studied animals [9]. Therefore,  $\text{BrO}_3^-$  removal from the water is an important issue from the last few decades. There are various methods for wastewater treatment including UV irradiation [10], ion exchange [11], reduction and adsorption using granular activated carbon [12,13] and granular ferric hydroxide [14], reduction using zero-valent iron ( $\text{Fe}^0$ ),  $\text{Fe}^{3+}$ , and  $\text{SO}_3$  [2,15–17], and filtration by reverse osmosis membrane [18]. All the above methods have their own merits and demerits which have been given in several papers [10–21]. Among all these methods, adsorption and ion exchange are the most effective and attractive techniques due to their low cost, high efficiency, and easy design [22–29].

This paper describes the removal of  $\text{BrO}_3^-$  using a strongly basic anion exchange resin Amberlite IRA-400 ( $\text{OH}^-$  form). Numerous operating parameters such as pH, contact time, temperature, and initial  $\text{BrO}_3^-$  concentration were investigated to find the optimum conditions for the adsorption process. Adsorption, desorption, and regeneration studies of Amberlite IRA-400 resin were studied. The analytical applicability of Amberlite IRA-400 resin was established for the  $\text{BrO}_3^-$  adsorption from bottled water and municipal water samples. The concentration of  $\text{BrO}_3^-$  in the water samples was determined by ultra-performance liquid chromatography–tandem mass spectrometry (UPLC–MS/MS) which is a very sensitive, precise, and rapid method [30].

## 2. Experimental

### 2.1. Chemicals and materials

Potassium bromate was purchased from BDH chemicals Ltd. (Poole, England) and formic acid was obtained from Panreac (Barcelona, Spain). The standard solutions of potassium bromate of various concentration levels ( $10\text{--}100\ \mu\text{g mL}^{-1}$ ) were prepared in Milli-Q water for calibration curves. Amberlite IRA-400 ( $\text{OH}^-$  form) was purchased from Sigma-Aldrich (USA). Water was purified through a Milli-Q water purification system (Millipore Corporation, Bedford, MA, USA). Other chemicals and reagents were of analytical reagent grade.

### 2.2. Chromatographic separation

The chromatographic separation of  $\text{BrO}_3^-$  was conducted using an UPLC technique, equipped with a quaternary pump system (Waters, Milford, MA,

USA). The analytical column was used an Acquity BEH  $\text{C}_{18}$  of dimension  $50 \times 2.1\ \text{mm}$  id and  $1.7\ \mu\text{m}$  particle size (Waters, Milford, MA, USA). The best possible separation was accomplished with a mobile phase consisting of 99.9% Milli-Q  $\text{H}_2\text{O}$  with 0.1% of formic acid. The flow rate of mobile phase and sample injection volume was  $200\ \mu\text{L min}^{-1}$  and  $5\ \mu\text{L}$ , respectively [30].

### 2.3. Mass spectrometric conditions

The UPLC technique was coupled to a Quattro Premier triple quadrupole mass spectrometer equipped with ESI source. The mass spectrometer instrument was used in negative ionization mode, and data were achieved in MRM form using the deprotonated molecular ion of  $\text{BrO}_3^-$  as a precursor ion. The ESI source working parameters were as follows: capillary voltage, 3.0 kV; cone voltage, 30 V; desolvation temperature,  $350\ ^\circ\text{C}$ ; source temperature,  $120\ ^\circ\text{C}$ ; desolvation gas flow rate,  $600\ \text{L h}^{-1}$ ; and cone gas flow rate,  $60\ \text{L h}^{-1}$ . Nitrogen (99.99% purity) and high-purity argon (99.99%) were applied as cone and collision gases, respectively. An Oerlikon rotary pump, model SOGEVAC SV40 BI (Paris, France) supplied the primary vacuum to the mass spectrometer. The optimum MS/MS conditions such as dwell times, collision energy voltages, and precursors and products ions related to the selected transitions for  $\text{BrO}_3^-$  are presented in Table 1. The most abundant product ion was observed to estimate the  $\text{BrO}_3^-$ , and the second most abundant product ion was observed to confirm the  $\text{BrO}_3^-$  identification. The data acquisition were achieved by MassLynx V4.1 software (Waters, Milford, MA, USA) [30].

### 2.4. Batch adsorption studies

Amberlite IRA-400 ( $\text{OH}^-$  form) was washed with Milli-Q water for five times to remove the stacked impurities from resin surface and dried in oven at  $50\ ^\circ\text{C}$  for 2 h. The adsorption of  $\text{BrO}_3^-$  on Amberlite IRA-400 resin was studied by batch experiments. The adsorption experiments were conducted in 100 mL conical flasks. In a conical flask, 50 mg of Amberlite IRA-400 was loaded with 50 mL  $\text{BrO}_3^-$  solution of known concentration which was kept in thermostat cum shaking assembly. The solution was shaken continuously at constant temperature for a certain time to get the equilibration time. After equilibration time, Amberlite IRA-400 was filtered off using Whatman filter No. 41. The concentrations of  $\text{BrO}_3^-$  in the solution phase before and after adsorption were determined by

Table 1  
MRM parameters used with the triple quadrupole instrument<sup>a</sup> [30]

Analyte	Precursor ion ( <i>m/z</i> )	Quantitation		Confirmation	
		Product ion ( <i>m/z</i> )	Collision energy (eV)	Product ion ( <i>m/z</i> )	Collision energy (eV)
BrO <sub>3</sub> <sup>-</sup>	128.85	112.85	22	116	26

<sup>a</sup>Dwell time was 0.1 s.

UPLC–MS/MS. Several parameters such as pH, contact time, initial BrO<sub>3</sub><sup>-</sup> concentration, and temperature were altered to optimize the adsorption process.

The amount of adsorbed BrO<sub>3</sub><sup>-</sup> at equilibrium,  $q_e$  (mg g<sup>-1</sup>) was computed as follows:

$$q_e = \frac{V(C_o - C_e)}{W} \quad (1)$$

where  $V$  is the volume of BrO<sub>3</sub><sup>-</sup> solution in litre,  $C_o$ , and  $C_e$  are the initial and final concentrations (mg L<sup>-1</sup>) of BrO<sub>3</sub><sup>-</sup> in solution, respectively,  $W$  is the weight (g) of Amberlite IRA-400.

Kinetics studies were accomplished by varying the bromate concentration ( $C_o$ , 500, 700, and 1,000 by µg L<sup>-1</sup>). Isotherm and thermodynamic studies were evaluated by varying initial concentration of BrO<sub>3</sub><sup>-</sup> solution (300–1,000 µg L<sup>-1</sup>) and temperature (20–55 °C).

### 2.5. Desorption and regeneration studies

For the desorption studies, 50 mL of 500 µg L<sup>-1</sup> BrO<sub>3</sub><sup>-</sup> solution was treated with 50 mg of Amberlite IRA-400 resin in flask at 120 revolution min<sup>-1</sup> for 1 h. After 1 h, Amberlite IRA-400 resin was filtered off and washed several times with Milli-Q water to remove the excess of bromate. Then, Amberlite IRA-400 resin was treated with 50 mL of 0.01 mol L<sup>-1</sup> NaOH solution in flask at aforementioned conditions. After 1 h, the solution was filtered and remaining concentration of BrO<sub>3</sub><sup>-</sup> in the solution was evaluated by UPLC–MS/MS.

The regeneration studies were also conducted by batch method. Amberlite IRA-400 resin (50 mg) was saturated with 500 µg L<sup>-1</sup> BrO<sub>3</sub><sup>-</sup> solution for 1 h. Subsequently, Amberlite IRA-400 resin was washed several times with Milli-Q water to remove unadsorbed bromate. To regenerate the saturated Amberlite IRA-400 resin, it was treated with 50 mL of 0.01 mol L<sup>-1</sup> NaOH solution. The same process was repeated for five consecutive cycles.

## 3. Results and discussion

Amberlite IRA-400, (OH<sup>-</sup> form) was used for the removal of BrO<sub>3</sub><sup>-</sup> which is a Group B2 substance

(probable human carcinogen). The equilibration time for the optimum adsorption of BrO<sub>3</sub><sup>-</sup> on Amberlite IRA-400 resin was conducted at different time intervals (5–60 min). It can be seen from Fig. 1(a) that the adsorption was fast at the beginning, and equilibrium was established at 40 min where 84.1% adsorption was found. The different rate of adsorption might be due to the fact that all resin sites were vacant at the starting. So the adsorption of BrO<sub>3</sub><sup>-</sup> was high. Later, owing to the decrease in the numbers of adsorption sites as well as BrO<sub>3</sub><sup>-</sup> concentration, the BrO<sub>3</sub><sup>-</sup> adsorption onto Amberlite IRA-400 became slow [31]. The effect of pH for the adsorption of BrO<sub>3</sub><sup>-</sup> using Amberlite IRA-400 resin was studied at pH range 2–7 pH meter (744, Metrohm, Switzerland). The removal of BrO<sub>3</sub><sup>-</sup> was increased from 39 to 85% with the increase in pH from 2 to 6.5 (Fig. 1(b)). From the above results, it was concluded that Amberlite IRA-400 resin could be effectively used at the neutral pH and there was no need to adjust the pH. The BrO<sub>3</sub><sup>-</sup> adsorption onto Amberlite IRA-400 resin was also studied by varying the BrO<sub>3</sub><sup>-</sup> concentration (200–1,000 µg L<sup>-1</sup>) at pH 6.5 for 40 min. The percentage removal of BrO<sub>3</sub><sup>-</sup> was decreased from 89 to 65% as the concentration of BrO<sub>3</sub><sup>-</sup> was increased from 200 to 1,000 µg L<sup>-1</sup>, which was owing to the less availability of adsorption sites at the surface of Amberlite IRA-400 resin for the higher dose of bromate (Fig. 1(c)). The effect of temperature was carried out by varying the temperature from 20 to 55 °C at pH 6.5 for 40 min (Fig. 1(d)). It was seen that the adsorption of BrO<sub>3</sub><sup>-</sup> was increased from 53.1 to 83.4% with the increase in temperature from 20 to 45 °C, which demonstrated the endothermic nature of BrO<sub>3</sub><sup>-</sup> adsorption onto Amberlite IRA-400 resin.

### 3.1. Adsorption kinetics

The pseudo-first-order equation [32] was given as:

$$\log(q_e - q_t) = \log q_e - \frac{k_1 t}{2.303} \quad (2)$$

where  $k_1$  (min<sup>-1</sup>) is the rate constant for pseudo-first-order,  $q_e$ , and  $q_t$  are the amounts of BrO<sub>3</sub><sup>-</sup> adsorbed at

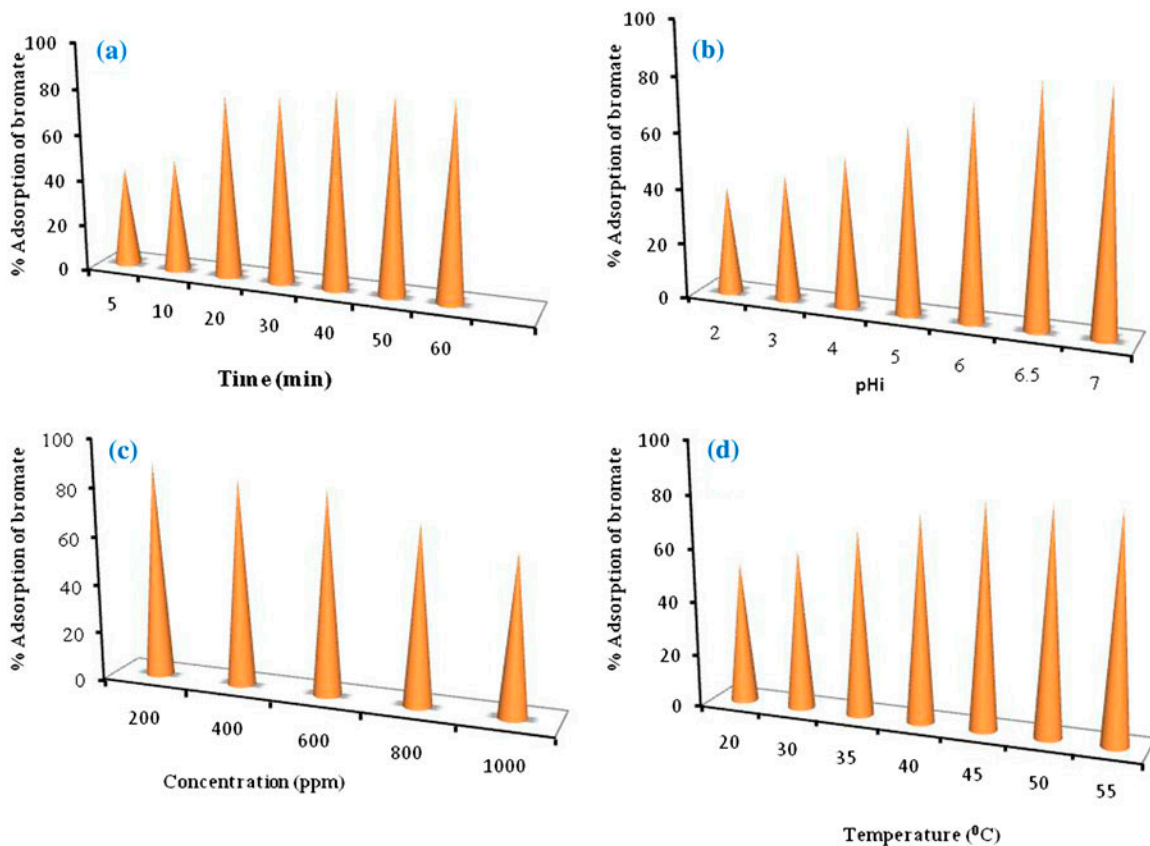


Fig. 1. Percent adsorption of bromate at different (a) time, (b) pH, (c) concentration, and (d) temperature; using Amberlite IRA-400 anion exchange resin.

equilibrium and time  $t$ , respectively. The values of  $k_1$  were calculated from the slope of the plot  $\log(q_e - qt)$  vs.  $t$ .

The pseudo-second-order kinetic rate equation [33] was given as:

$$\frac{t}{q_t} = \frac{1}{k_2 q_e^2} + \frac{t}{q_e} \quad (3)$$

where  $k_2$  is the pseudo-second-order rate constant and its values were determined from the intercepts of the plot  $t/q_t$  vs. time. The obtained parameters for these two models are shown in Table 2. The values of correlation coefficients ( $R^2$ ) for pseudo-second-order model were found to be higher than pseudo-first-order model, which showed that pseudo-second-order model was well fitted (Fig. 2(a) and (b)).

### 3.2. Adsorption isotherms

The Langmuir isotherm [34] model can be expressed as:

$$\frac{1}{q_e} = \frac{1}{Q_0} + \frac{1}{bQ_0C_e} \quad (4)$$

where  $C_e$  is the equilibrium concentration of  $\text{BrO}_3^-$ ,  $q_e$  is the amount of adsorbed  $\text{BrO}_3^-$ ,  $Q_0$  and  $b$  are the Langmuir constants and the values of  $Q_0$ , and  $b$  were obtained from the intercept and slope of linear plots of  $1/q_e$  vs.  $1/C_e$ , respectively (Table 3).

In order to calculate the adsorption effectiveness of the adsorption process, the separation factor ( $R_L$ ) was determined by using the following equation [35]:

$$R_L = \frac{1}{1 + K_L C_0} \quad (5)$$

where  $K_L$  is the Langmuir adsorption constant and  $C_0$  is the lowest initial concentration of  $\text{BrO}_3^-$ . The value of  $R_L$  confirms whether the adsorption is linear ( $R_L = 1$ ), unfavorable ( $R_L > 1$ ), favorable ( $0 < R_L < 1$ ), or irreversible ( $R_L = 0$ ). In the present study, the values of  $R_L$  were greater than zero and less than unity

Table 2

Kinetic parameters obtained for the adsorption of bromate onto Amberlite IRA-400 anion exchange resin

Initial concentration of bromated ( $\mu\text{g L}^{-1}$ )	Pseudo-first-order				Pseudo-second-order			
	Slope	Intercept	$k_1$ ( $\text{min}^{-1}$ )	$R^2$	Slope	Intercept	$k_2$ ( $\text{g mg}^{-1} \text{min}^{-1}$ )	$R^2$
500	-0.0506	2.59	$11.65 \times 10^{-2}$	0.918	0.0021	0.0129	$3.42 \times 10^{-4}$	0.992
700	-0.0508	2.74	$11.69 \times 10^{-2}$	0.920	0.0016	0.0103	$2.49 \times 10^{-4}$	0.990
1,000	-0.0508	2.91	$11.69 \times 10^{-2}$	0.930	0.0011	0.0082	$1.48 \times 10^{-4}$	0.990

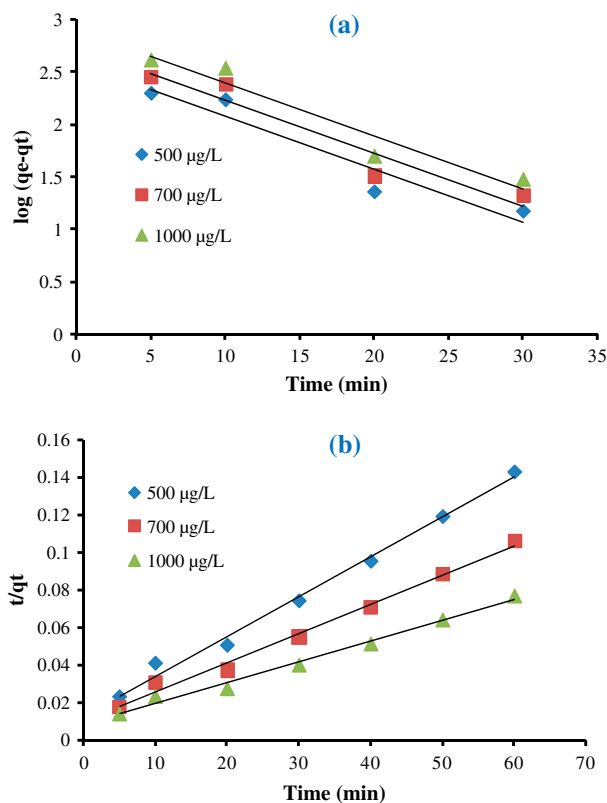


Fig. 2. Plots of kinetic models (a) pseudo-first-order and (b) pseudo-second-order for the adsorption of bromate by Amberlite IRA-400 anion exchange resin.

which designated the favorable adsorption of  $\text{BrO}_3^-$  onto Amberlite IRA-400 resin.

Table 3

Adsorption isotherm parameters for bromate adsorption onto Amberlite IRA-400 anion exchange resin

Temperature ( $^{\circ}\text{C}$ )	Langmuir constants			Freundlich constants			
	$Q_m$ ( $\text{mg g}^{-1}$ )	$b$ ( $\text{L mg}^{-1}$ )	$R^2$	$1/n$	$n$	$K_f$	$R^2$
20	1.99	0.57	0.941	0.653	1.53	1.74	0.999
30	1.88	0.82	0.952	0.672	1.49	1.37	0.997
50	1.49	2.99	0.935	0.673	1.48	1.18	0.998

The Freundlich isotherm is expressed as:

$$\log q_e = \log K_f + \frac{1}{n} \log C_e \quad (6)$$

where  $K_f$  and  $n$  are the Freundlich isotherm constants and their values were obtained from the slope ( $1/n$ ) and intercept ( $\log K_f$ ) the plot of  $\log q_e$  vs.  $\log C_e$ , respectively. The value of  $n$  is an indication of the feasibility of adsorption. Values of  $n > 1$  show favorable nature of adsorption. The value of  $n > 1$  for  $\text{BrO}_3^-$  adsorption onto Amberlite IRA-400 resin indicated the favorable adsorption at different concentrations. The parameters derived by applying these two models (Fig. 3(a) and (b)) are given in Table 3. The Freundlich model showed the better correlation coefficient values ( $R^2 > 0.99$ ), which demonstrated the better applicability of this model.

A comparison of maximum monolayer adsorption capacity of  $\text{BrO}_3^-$  on various adsorbents [14,21,36,37] was carried out and it was found that the maximum monolayer adsorption capacity of Amberlite IRA-400 resin for  $\text{BrO}_3^-$  was higher than other adsorbents.

### 3.3. Thermodynamic studies

The thermodynamic parameters,  $\Delta G^{\circ}$  (standard free energy),  $\Delta H^{\circ}$  (enthalpy change), and  $\Delta S^{\circ}$  (entropy change) were evaluated to determine the feasibility and nature of adsorption process. The values of  $\Delta H^{\circ}$  and  $\Delta S^{\circ}$  were calculated from the slopes and intercepts of the plots of  $\ln K_c$  vs.  $1/T$  (Fig. 4) by using the following equation.

$$\ln K_c = -\frac{\Delta H^{\circ}}{RT} + \frac{\Delta S^{\circ}}{R} \quad (7)$$

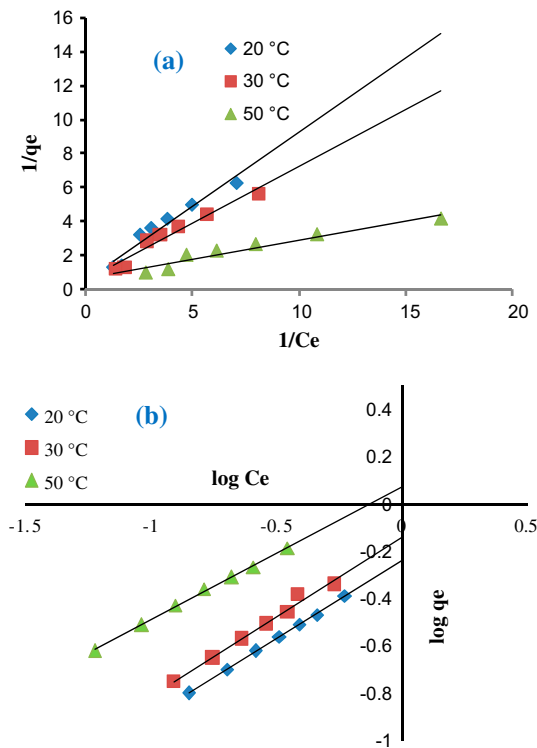


Fig. 3. Plots of isotherm models (a) Langmuir and (b) Freundlich for the adsorption of bromate by Amberlite IRA-400 anion exchange resin.

The  $\Delta G^\circ$  (free energy change) was calculated from the following relation.

$$\Delta G^\circ = \Delta H^\circ - T\Delta S^\circ \quad (8)$$

where  $R$  is the gas constant,  $T$  (K) is the absolute temperature, and  $K_c$  ( $\text{L mg}^{-1}$ ) is the standard thermodynamic equilibrium constant defined by  $q_e/C_e$ . The values of  $\Delta G^\circ$  and  $\Delta H^\circ$ ,  $\Delta S^\circ$ , for  $\text{BrO}_3^-$  adsorption onto Amberlite IRA-400 resin are given in Table 4. It is apparent from Table 4 that the values of  $\Delta H^\circ$  was positive showed the endothermic nature of the adsorption. The positive values of  $\Delta S^\circ$  reflected an increase in the randomness at the solid/solution

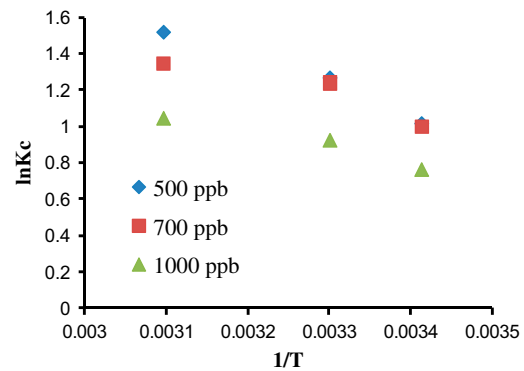


Fig. 4. Van't Hoff plot  $\ln K_c$  vs.  $1/T$  for the adsorption of bromate by Amberlite IRA-400.

interface during the adsorption process. The negative values of  $\Delta G^\circ$  indicated the degree of spontaneity of the adsorption process.

#### 3.4. Desorption of $\text{BrO}_3^-$ and regeneration of Amberlite IRA-400 resin

Regeneration is one of the most important factors in the applicability of the adsorbents. In the present study, when the Amberlite IRA-400 resin was saturated by  $\text{BrO}_3^-$  anions, it was regenerated using  $0.1 \text{ mol L}^{-1}$  NaOH solution. It is clear from Fig. 5 that the adsorption was reduced from 84 to 62.8% and the recovery was reduced from 79 to 61.2% after five sequential cycles, indicated the excellent adsorption stability of Amberlite IRA-400 resin.

#### 3.5. Analytical applications for real water samples

Municipal water samples were obtained in a clear glass bottles (250 mL) from local district supplied by the national company Saline Water Conversion Corporation, Saudi Arabia. Bottled drinking water (non-carbonated) of different brands was obtained from a local super market in Riyadh, Saudi Arabia. The samples were filtered through  $0.20 \mu\text{m}$  PTFE syringe

Table 4  
Thermodynamics parameters for bromate adsorption onto Amberlite IRA-400 anion exchange resin

$C_o, \mu\text{g L}^{-1}$	$\Delta H^\circ, \text{J mol}^{-1}$	$\Delta S^\circ, \text{J mol}^{-1} \text{K}^{-1}$	$\Delta G^\circ, \text{J mol}^{-1}$		
			293 K	303 K	323 K
500	12.77	0.052	-5.86	-1.79	-0.49
700	8.31	0.037	-7.00	-2.93	-1.64
1,000	7.11	0.031	-8.21	-4.13	-2.84

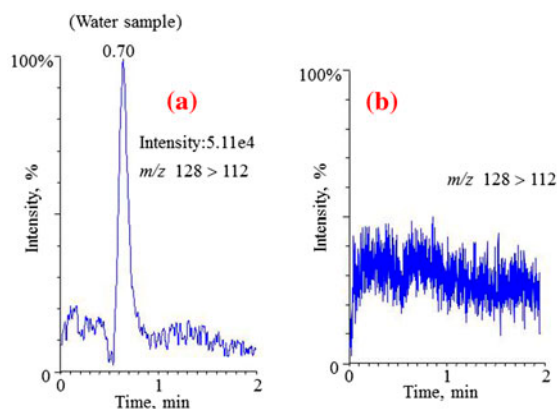


Fig. 5. UPLC–MS chromatograms of bromate in water sample (a) before adsorption and (b) after adsorption.

filter prior to UPLC–MS/MS injection. The  $\text{BrO}_3^-$  concentration water was labeled ( $<10 \mu\text{g L}^{-1}$ ) in each bottled by the relevant companies. Each water sample (20 mL) was taken in conical flask and shaken with 0.2 g of Amberlite IRA-400 resin at optimum conditions (pH 6.5, time 40 min and temperature  $45^\circ\text{C}$ ) in a thermostated shaker. After equilibration time, the water samples were taken out from the shaker and filtered through 0.22 mm PVDF filter before being injected into UPLC–MS system. It can be seen from Fig. 5 that the  $\text{BrO}_3^-$  peak was at the retention time of 0.4 min before adsorption which was completely diminished after adsorption.

#### 4. Conclusions

From the above-mentioned experimental results, the following conclusions were found:

- (1) Adsorption of  $\text{BrO}_3^-$  by Amberlite IRA-400 anion exchange resin was fast and the equilibrium established within 40 min.
- (2) The maximum monolayer adsorption capacity ( $Q_m$ ) was  $1.9 \text{ mg g}^{-1}$  at  $20^\circ\text{C}$  which was higher than other adsorbents studied here.
- (3) The adsorption kinetics and isotherms were well fitted by pseudo-second-order model and Freundlich model, respectively.
- (4) Amberlite IRA-400 anion exchange resin could be effectively used up to five cycles.

#### Acknowledgement

This work was supported by NSTIP strategic technologies program number (12-WAT 3138-02) in the Kingdom of Saudi Arabia.

#### References

- [1] EPA, Disinfection Byproduct Information, Information Collection Rule, Office of Ground Water and Drinking Water, US Environmental Protection Agency, Washington, DC, 2006. Available from: <http://www.epa.gov/enviro/html/icr/dbp.html>.
- [2] J. Kemsley, Bromate in Los Angeles water, Chem. Eng. News 85 (52) (2008) 9. Available from: <http://pubs3.acs.org/cen/news/85/i52/8552notw4.html>.
- [3] G. Amy, C. Douville, B. Daw, J. Sohn, C. Galey, D. Gatel, J. Cavard, Bromate formation under ozonation conditions to inactivate cryptosporidium, Water Sci. Technol. 41 (2009) 61–66.
- [4] Y. Zhong, Q. Yang, K. Luo, X. Wu, X. Li, Y. Liu, W. Tang, G. Zeng, B. Peng, Fe(II)–Al(III) layered double hydroxides prepared by ultrasound-assisted co-precipitation method for the reduction of bromate, J. Hazard. Mater. 250 (2013) 345–353.
- [5] T. Umemura, Y. Kurokawa, Etiology of bromate-induced cancer and possible modes of action-studies in Japan, Toxicology 221 (2006) 154–157.
- [6] A.M.V.D. Looijaard, J.V. Genderen, Levels of exposure from drinking water, Food Chem. Toxicol. 38 (2000) 37–42.
- [7] K.C. Campbell, Bromate-induced ototoxicity, Toxicology 221 (2006) 205–211.
- [8] US EPA, National primary drinking water regulations: Disinfectants and disinfection by-products, Federal Register 63, Washington, DC, 1998, pp. 69405–69411.
- [9] International Agency for Research on Cancer (IARC), Monographs on the Evaluation of Carcinogenic Risks to Humans, Potassium Bromate (Group 2 B), IARC, Lyon, France, 2006.
- [10] S. Peldszus, S.A. Andrews, R. Souza, F. Smith, I. Douglas, J. Bolton, P.M. Huck, Effect of medium-pressure UV irradiation on bromate concentrations in drinking water, a pilot-scale study, Water Res. 38 (2004) 211–217.
- [11] P.C. Singer, K. Bilyk, Enhanced coagulation using a magnetic ion exchange resin, Water Res. 36 (2002) 4009–4022.
- [12] M.J. Kirisits, V.L. Snoeyink, J.C. Kruithof, The reduction of bromate by granular activated carbon, Water Res. 34 (2000) 4250–4260.
- [13] W.F. Chen, Z. Zhang, Q. Li, H.Y. Wang, Adsorption of bromate and competition from oxyanions on cationic surfactant-modified granular activated carbon (GAC), Chem. Eng. J. 203 (2012) 319–325.
- [14] A. Bhatnagar, Y. Choi, Y.J. Yoon, Y. Shin, B.H. Jeon, J.W. Kang, Bromate removal from water by granular ferric hydroxide (GFH), J. Hazard. Mater. 170 (2009) 134–140.
- [15] L. Xie, C. Shang, Effects of copper and palladium on the reduction of bromate by Fe(0), Chemosphere 64 (2006) 919–930.
- [16] L. Xie, C. Shang, Q. Zhou, Effect of Fe(III) on the bromate reduction by humic substances in aqueous solution, J. Environ. Sci. 20 (2008) 257–261.
- [17] G. Gordon, R.D. Gauw, G.L. Emmert, B.D. Walters, B. Bubnis, Chemical reduction methods for bromate ion removal, J. Am. Water Works Assoc. 94 (2002) 91–98.
- [18] V.S. Hatzistavros, P.E. Koulouridakis, I.I. Aretaki, N.G.K. Kontos, Bromate determination in water after

- membrane complexation and total reflection X-ray fluorescence analysis, *Anal. Chem.* 79 (2007) 2827–2832.
- [19] B. Ozkahraman, A. Bal, I. Acar, G. Guclu, Adsorption of brilliant green from aqueous solutions onto cross-linked chitosan graft copolymers, *Clean-Soil, Air, Water* 39 (2011) 1001–1006.
- [20] T.K. Saha, N.C. Bhoumik, S. Karmaker, M.G. Ahmed, H. Ichikawa, Y. Fukumori, Adsorption characteristics of reactive black 5 from aqueous solution onto chitosan, *Clean-Soil, Air, Water* 39 (2011) 984–993.
- [21] M. Naushad, Z.A. ALOthman, M.R. Khan, S.M. Wabaidur, Removal of bromate from water using De-Acidite FF-IP resin and determination by ultra-performance liquid chromatography–tandem mass spectrometry, *Clean-Soil Air Water* 41 (2013) 528–533.
- [22] A. Mittal, V. Thakur, J. Mittal, H. Vardhan, Process development for the removal of hazardous anionic azo dye Congo red from wastewater by using hen feather as potential adsorbent, *Desalin. Water Treat.* 52 (2014) 227–237.
- [23] S.M. Alshehri, Mu. Naushad, T. Ahmad, Z.A. ALOthman, A. Aldalbahi, Synthesis, characterization of curcumin based ecofriendly antimicrobial bio-adsorbent for the removal of phenol from aqueous medium, *Chem. Eng. J.* 254 (2014) 181–189.
- [24] H. Daraei, A. Mittal, J. Mittal, H. Kamali, Optimization of Cr(VI) removal onto biosorbent eggshell membrane: Experimental & theoretical approaches, *Desalin. Water Treat.* 52 (2014) 1307–1315.
- [25] A. Mittal, Use of hen feathers as potential adsorbent for the removal of a hazardous dye, Brilliant Blue FCF, from wastewater, *J. Hazard. Mater.* 128 (2006) 233–239.
- [26] R. Jain, M. Mathur, S. Sikarwar, A. Mittal, Removal of the hazardous dye rhodamine B through photocatalytic and adsorption treatments, *J. Environ. Manage.* 85 (2007) 956–964.
- [27] V.K. Gupta, R. Jain, A. Mittal, T.A. Saleh, A. Nayak, S. Agarwal, S. Sikarwar, Photo-catalytic degradation of toxic dye amaranth on TiO<sub>2</sub>/UV in aqueous suspensions, *Mater. Sci. Eng., C* 32 (2012) 12–17.
- [28] V.K. Gupta, A. Mittal, R. Jain, M. Mathur, S. Sikarwar, Adsorption of Safranin-T from wastewater using waste materials-activated carbon and activated rice husks, *J. Colloid Interface Sci.* 303 (2006) 80–86.
- [29] J. Mittal, V. Thakur, A. Mittal, Batch removal of hazardous azo dye Bismark Brown R using waste material hen feather, *Ecol. Eng.* 60 (2013) 249–253.
- [30] I.H. Alsohaimi, Z.A. ALOthman, M.R. Khan, M.A. Abdalla, A.K. Alomary, R. Busquets, Determination of bromate in drinking water by ultraperformance liquid chromatography–tandem mass spectrometry, *J. Sep. Sci.* 35 (2012) 2538–2543.
- [31] M. Naushad, Z.A. ALOthman, M. Islam, Adsorption of cadmium ion using a new composite cation-exchanger polyaniline Sn (IV) silicate: Kinetics, thermodynamic and isotherm studies, *Int. J. Environ. Sci. Technol.* 10 (2013) 567–578.
- [32] S. Lagergren, About the theory of so-called adsorption of soluble substances, *KungligaSvenskaVetenskapsakademiens. Handlingar, Band 24* (1898) 1–39.
- [33] Y.S. Ho, G.M. Kay, Sorption of dye from aqueous solution by peat, *Chem. Eng. J.* 70 (1998) 115–124.
- [34] I. Langmuir, The constitution and fundamental properties of solids and liquids. Part I. Solids, *J. Am. Chem. Soc.* 38 (1916) 2221–2295.
- [35] M. Naushad, Surfactant assisted nano-composite cation exchanger: Development, characterization and applications for the removal of toxic Pb<sup>2+</sup> from aqueous medium, *Chem. Eng. J.* 235 (2014) 100–108.
- [36] C. Xu, J. Shi, W. Zhou, B. Gao, Q. Yue, X. Wang, Bromate removal from aqueous solutions by nano crystalline akaganeite (β-FeOOH)-coated quartz sand (CACQS), *Chem. Eng. J.* 187 (2012) 63–68.
- [37] L. Wang, J. Zhang, J. Liu, H. He, M. Yang, J. Yu, Z. Ma, F. Jiang, Removal of bromate ion using powdered activated carbon, *J. Environ. Sci.* 22 (2010) 1846–1853.